Electronic Supplementary Material (ESI) for Journal of Materials Chemistry B.
This journal is © The Royal Society of Chemistry 2018

Supporting information

Shape-shifting composite hydrogel sheet with spatially patterned plasmonic nanoparticles

Hongyu Guo[a], Yijing Liu[b], Yang Yang[a], Guangyu Wu[a,c], Kerry Demella[d], Srinivasa R. Raghavan[d] and Zhihong Nie[a*]

[a]Department of Chemistry and Biochemistry, University of Maryland, College Park, MD 20742, USA

[b]Laboratory of Molecular Imaging and Nanomedicine (LOMIN), National Institute of Biomedical Imaging and Bioengineering (NIBIB), National Institutes of Health, USA

[c]MIIT Key Laboratory of Critical Materials Technology for New Energy Conversion and Storage, State Key Laboratory of Urban Water Resource and Environment, School of Chemistry and Chemical Engineering, Harbin Institute of Technology, Harbin 150001, China

[d]Department of Chemical and Biomolecular Engineering, University of Maryland, College Park, MD 20742, USA

* Corresponding author. E-mail: znie@umd.edu

Experimental section

Materials. All chemicals were purchased from Sigma-Aldrich unless otherwise noted and the chemicals were used without further treatment. Chemicals used were as follows: N-Isopropylacrylamide (NIPAM, monomer), N,N'-Methylenebis(acrylamide) (BIS, cross-linker,), Ammonium persulfate (APS, initiator), N,N,N',N'-Tetramethylethylenediamine (TEMED, catalyst), Silver nitrate ($AgNO_3$), Polyvinylpyrrolidone (PVP, MW 55000), Gold(III) chloride trihydrate ($HAuCl_4$), Ethylene glycol (EG), Ammonium hydroxide (25.0%-28.0%). Hydrogen peroxide (30% solution) was purchased from EMD Millipore Cooperation. Agarose powder was purchased from EZ BioResearch. Polydimethylsiloxane (PDMS) elastomer kit (Sylgard 184) was bought from Dow Corning. Deionized water was used throughout the experiments.

Synthesis of Silver Nanoparticle (AgNP). Silver nanoparticle was synthesized according to ref.1 (Synthesis of Ag Seeds section) in this supporting information.

Synthesis of AgNP-Loaded Hydrogel. The AgNP-loaded hydrogel was fabricated by a redox method. Typically, 0.113g NIPAM monomer and 0.008g BIS cross-linker were dissolved in 500 μL AgNP aqueous solution. After adding 5 μL 10 wt% APS aqueous solution, the hydrogel precursor solution was put on ice bed for 5 minutes. Then 0.1 μL TEMED was added and mixed with the monomer solution. After mixing, the monomer solution was injected into a pre-made mold made of two glass slides and a spacer. The gelation took place at room temperature in a few minutes and the glass mold was then put in 4 °C refrigerator for the gelation to proceed further for 2 hours. After 2 hours, the glass mold was immersed in water and was open to release the AgNP-loaded hydrogel. The AgNP-loaded hydrogel was kept in a large amount of water for one day to leak out unreacted chemicals.

Fabrication of Agarose Stamp. The agarose stamp was made by gelating agarose aqueous solution on a PDMS mold. In a representative fabrication process, a poly(lactic acid) (PLA) plastic mold with bas-relief features was first printed out by using 3D printer (Original Prusa i3 MK2S).

Then PDMS was cured on this mold at 70 °C for 1 hour. The cured PDMS with opposite features was peeled off from PLA mold. After that, the PDMS mold surface was made hydrophilic by subjecting it to air plasma for three minutes. Then 4 wt% hot agarose aqueous solution was casted onto PDMS mold and cooled at room temperature to gelate. After gelation, the agarose gel with bas-relief features was peeled off from the PDMS mold. This agarose gel was then used in wet stamping process.

Wet Stamping. The agarose gel with base-relief features was first immersed in gold precursor ($HAuCl_4$) aqueous solution for 30 minutes. Then it was taken out and the $HAuCl_4$ precursor on agarose gel surface was removed by using Kimwipes. The agarose stamp was then brought into contact with the surface of AgNP-loaded hydrogel. Once agarose stamp was in contact with AgNP-loaded hydrogel, galvanic replacement reaction between $HAuCl_4$ and AgNP started and gold nanoparticle (AuNP) was generated *in-situ*. By designing features in agarose stamp, different pattern forms of AuNP domains in the hydrogel could be easily obtained. After wet stamping, the unreacted AgNP in the hydrogel was etched away by using an aqueous mixture of ammonium hydroxide and hydrogen peroxide (6:1 in volume ratio), leaving behind AuNP domains in the hydrogel. Without special notification, we used hybrid hydrogel to represent AuNP-containing hydrogel. For fabricating agarose stamp loaded with gold ion of different concentrations, the PDMS mold used to make agarose stamp was utilized as an ink well. Aqueous gold ion solution with different concentrations were injected to the ink well. Then the agarose stamp was aligned with the ink well and was brought in contact with the gold ion solution to absorb gold ions. Finally the stamp was made in contact with AgNP-loaded hydrogel to generate gold nanoparticle domains of various sizes in both xy- and z-direction of the hydrogel.

Diffusion Study. The agarose stamp was brought in contact with the AgNP-loaded hydrogel for different amount of time. Then the AgNP was etched away. The size of the generated nanoparticle domain in both xy- and z-direction of the hydrogel was then analyzed by using optical microscope. The nanoparticle domain size was plotted with respect to stamping time.

Light-Triggered Shape Transformation. An 808 nm laser (MDL-N-808, Changchun New Industries Optoelectronics Technology Co., Ltd, China) with tunable output power (0-8W) was used as the laser source throughout the experiments. During the experiments, the hybrid hydrogel was immersed in 600 mL water in a glass petri dish.

Hydrogel Swelling. The swelling property of the hydrogel was characterized by using the swelling ratio which was measured gravimetrically after wiping off the excess water on the hydrogel's surface with a piece of Kim wipe in the temperature range from 18 to 36 °C. The hydrogel was incubated in a water bath for at least 24 h at each temperature. The swelling ratio was calculated by using the following formula,

$$\text{Swelling ratio} = W_s/W_d$$

where W_s was the weight of the swollen hydrogel at the particular temperature and W_d was the dry weight of the hydrogel.

Mechanical Property. An AR2000 stress-controlled rheometer (TA Instruments) was used to study the mechanical properties of the hybrid hydrogel sheet. Rheological experiments were performed at 25 °C, 28 °C and 35 °C, respectively by using cone-and-plate geometry (20 mm diameter and 2^{o} cone angle). A solvent trap was used to minimize drying of the sample during measurements. Dynamic stress-sweep experiments were first performed on the sample to identify its linear viscoelastic (LVE) region at different temperatures and dynamic frequency sweeps were then performed within the LVE region.

UV-VIS Measurement. The optical property of the hydrogel was characterized by measuring its light extinction using UV-VIS spectroscopy (Lambda 40 UV/VIS Spectrometer, PerkinElmer, USA). In the measurement, air was used as reference and a piece of hydrogel was then put on a glass slide. The UV-VIS spectra were then taken at a slit width of 1 nm, scanning speed of 480 nm/min and data interval of 1 nm.

Scanning Electron Microscopy (SEM). For silver nanoparticle (AgNP) characterization, a drop of AgNP aqueous solution was dried on silicon wafer and the dried sample was imaged by using scanning electron microscopy (XL Series-30, Philips, USA). For hybrid hydrogel characterization, the hybrid hydrogel was first freeze-dried and then coated with carbon (JFC-1200 Fine Coater, Japan). Following that, scanning electron microscopy was used to characterize AuNP in the hydrogel.

Photothermal Imaging of Hybrid Hydrogel. The photothermal property of the hybrid hydrogel was studied by photothermal imaging technique. Briefly, the hybrid hydrogel sheet was immersed in 3 mL water in a plastic petri dish and was irradiated with an 808 nm laser at a power density of 6.37 W/cm^2 for 1 min and then the laser was shut off. The surface temperature of the hybrid hydrogel was monitored by using a FLIR SC300 infrared camera (FLIR, Arlington, VA). Real-time thermal images were captured with frame rate at 60 Hz, and analyzed by FLIR Examiner software. We found that the hybrid hydrogel sheet started to deform while its surface temperature increased from 22 °C to 29 °C (Fig.S5a) during the irradiation process and it went back to its original shape when it cooled down.

Surface temperature of pure and hybrid PNIPAM hydrogel under laser irradiation. In the experiment, a piece of pure PNIPAM hydrogel (length: 25mm, width: 20mm, thickness: 2mm) was put on a plastic petri dish (made of polystyrene) in air at room temperature (18.5^{o}C). The hydrogel was irradiated by laser with different power densities for 1 minute. Then the laser was switched off and the surface temperature of the pure hydrogel was measured by using a digital thermometer (MeasuPro Waterproof Digital Food Thermometer). The correlation between surface temperature and laser power density is then plotted. For control experiment, a piece of hybrid PNIPAM hydrogel (length: 30mm, width: 25mm, thickness: 2mm) was also irradiated in air and its surface temperature was measured in the same way as pure hydrogel.

Jumping and Load-lifting of Composite Hydrogel Sheet. The composite hydrogel sheet (length: 20mm, width: 2mm, thickness: 0.25mm) was patterned with two AuNP strips (width: 2mm, thickness: 0.06mm) and it was irradiated by laser. The patterned hydrogel deformed and jumped by releasing the stored energy during its deformation (SV3). The patterned hydrogel was used to lift up load. A 3mg gelatin bead was raised to 1cm high by 18mg composite hydrogel sheet in 30 seconds under laser irradiation (SV4).

Estimation of Minimum Laser Energy Required for Bending to Occur. The composite hydrogel sheet ((length: 20mm, width: 2.2mm, thickness: 0.25mm)) was patterned with AuNP strip as the "hinge" in bending under irradiation. The width of AuNP was 2.2mm, while its length varied. We found that a larger laser power density was needed to initiate bending of composite sheet with a smaller hinge width in water (Fig. S14). We estimated the minimum laser energy (*E*) required for bending to occur by using the following equation,

$$E = (I_o - I_o * 10)wlt$$

where I_o, *Abs, t, w, l* are the intensity of incoming laser, absorbance of hydrogel sheet, onset time of bending, hinge width and length, respectively. Using this equation, E was calculated to be 0.9 J for this hydrogel (see Table S1).

Estimation of AgNP loading in original hydrogel. Loading of AgNP in the original hydrogel is estimated as follows. 0.1g $AgNO_3$ is assumed to be fully reduced to AgNP which is dispersed in 5mL. The mass of silver atom in the 5mL solution is $\frac{0.1g}{169.87g/mol} \times \frac{107.87g}{mol} = 0.0635g$. The volume ($V$) of a single AgNP with a diameter (d) of around 80nm (Fig. S2) is,

$$V = \frac{4}{3}\pi(\frac{d}{2})^3 = 2.1 \times 10^{-17}\ cm^3\ or\ mL$$

and mass (m) of a single AgNP is $m = \rho_{density}V = \frac{10.53g}{mL} \times 2.1 \times 10^{-17}mL = 2.3 \times 10^{-14}g$.

Then the number (N) of AgNP in 5mL solution is $N = \frac{0.0635g}{2.3 \times 10^{-14}g} = 2.8 \times 10^{12}$

The number density (N_v) of AgNP in solution is $Nv = \frac{N}{5mL} = \frac{2.8 \times 10^{12}}{5mL} = 5.6 \times 10^{11}/mL$.

Since one AgNP leads to one AuNP during galvanic replacement, the number density of AuNP in the composite hydrogel will be equal to $5.6 \times 10^{11}/mL$.

Estimation of magnitude change of modulus ratio (*e*) on bending curvature of composite hydrogel sheet. We examined the effect of modulus ratio, *e*, on bending curvature of the composite hydrogel sheet by using the model presented in the manuscript. We found that the magnitude change of *e* does not produce substantial effect on bending curvature of the composite hydrogel sheet, which agreed with the conclusion drawn in ref. 56 in the revised manuscript. The shear modulus of composite hydrogel sheet (active gel layer) as a function of temperature is shown in Table S2 and Fig. S5d, while the shear modulus of passive gel layer is 838 Pa (Table S2 and Fig. S15) at 25 °C. Shear modulus ratio is used to represent Young's modulus ratio (*e*) used in the model. The calculation result is shown below for the case when h=0.3 (h_{total}=0.25mm).

The model says,

$$\kappa = 6\frac{eh(1+h)\Delta\xi}{h_{total}(1 + 4eh + 6eh^2 + 4eh^3 + e^2h^4)} = A\Delta\xi$$

Here we write $\kappa = A\Delta\xi$ to evaluate the contribution of *e* (related to *A*) and $\Delta\xi$ to bending curvature κ.

Data used in calculation is shown in Table S3. The calculation result is shown in Table S4.

As seen from Table S4, the significant increase of bending curvature κ (from 1.79 to 11.13) when increasing temperature (from 28°C to 35°C) in hybrid gel layer at h=0.3 (corresponding to increasing laser power density) is because of great increase of $\Delta\xi$ (from 0.43 to 2.5), instead of magnitude change of e (from 2.65 to 4.58). This suggested that magnitude change of e during laser irradiation does not produce substantial effect on bending curvature of composite hydrogel sheet.

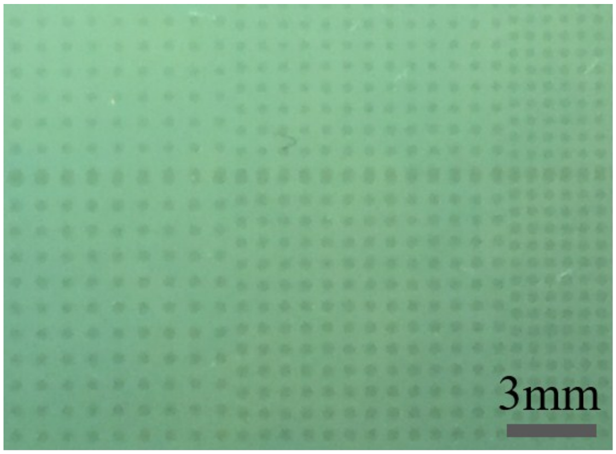

Fig. S1 Large-scale patterning of gold nanoparticles via stamping approach.

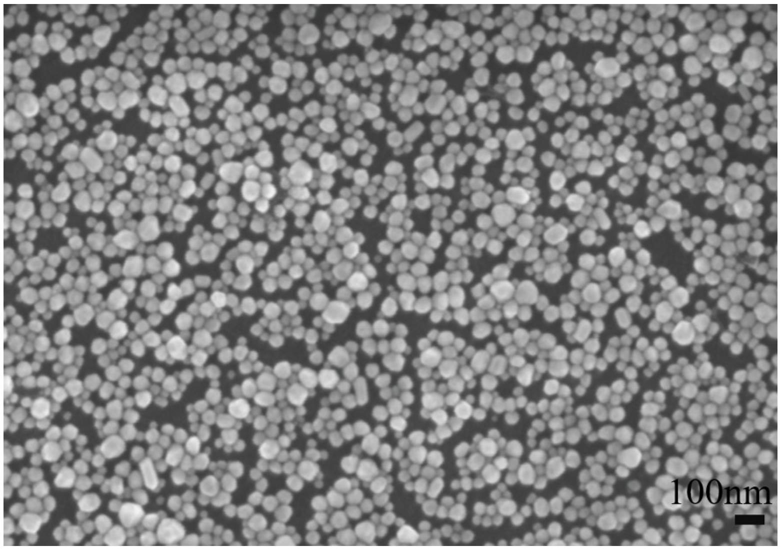

Fig. S2 SEM image of AgNP used to generate AuNP during stamping process.

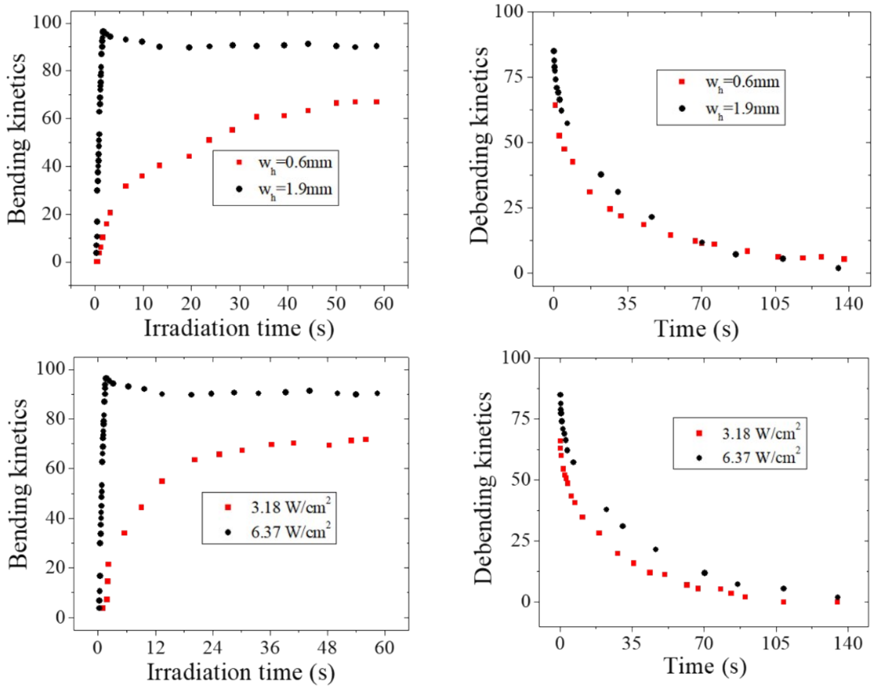

a b

Fig. S3 Bending and recovering kinetics of composite hydrogel with time. w_h was the width of gold nanoparticle domain. The length of gold nanoparticle domain was 2.2mm.

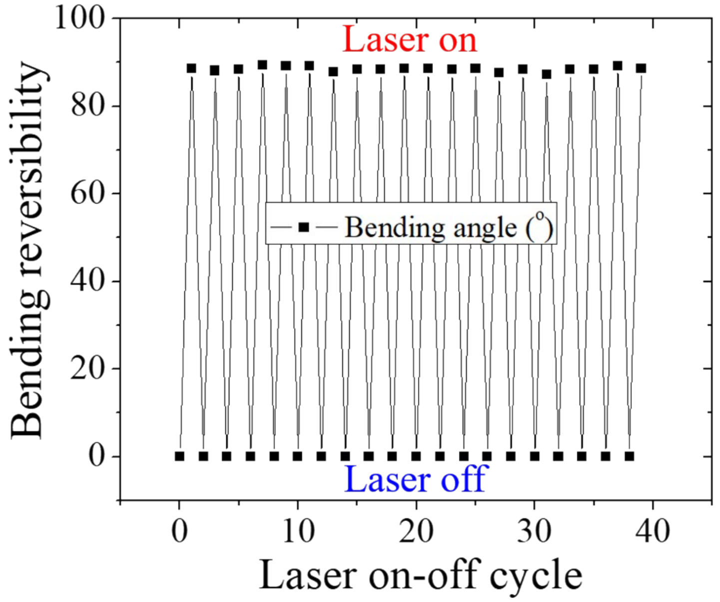

Fig. S4 Bending reversibility of composite hydrogel during laser on-off cycle

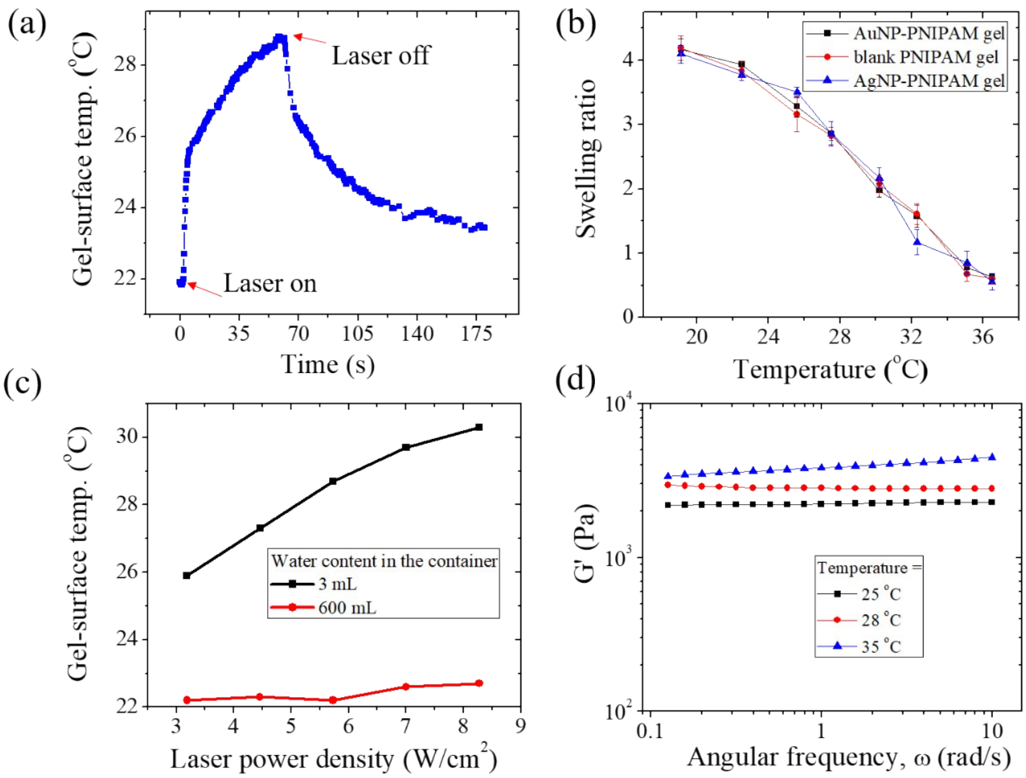

Fig. S5 a) Evolution of surface temperature of composite hydrogel during laser irradiation; b) Swelling of hydrogel as a function of temperature; c) Surface temperature of composite hydrogel as a function of laser power density; d) Shear modulus of composite hydrogel as a function of temperature.

Fig. S6 Bending of composite hydrogel with different thicknesses. The thickness of the composite hydrogel in a) is 0.25mm while it is 0.5mm in b). Thickness of hybrid gel layer is 0.06mm in a) and 0.12mm in b). Scale bar: 2mm.

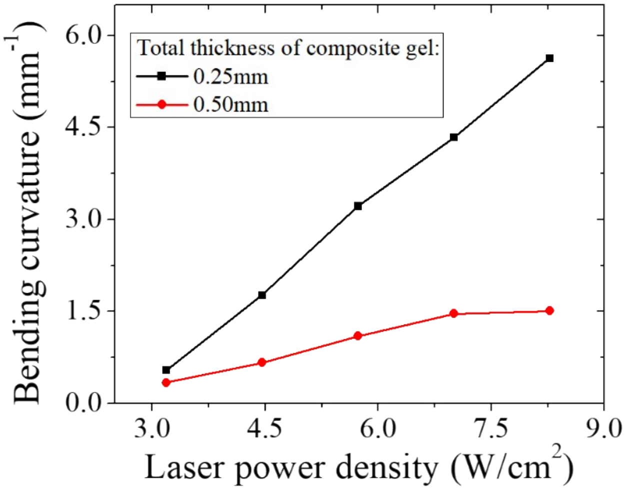

Fig. S7 Quantitative analyses of bending curvature of composite hydrogel with different thicknesses.

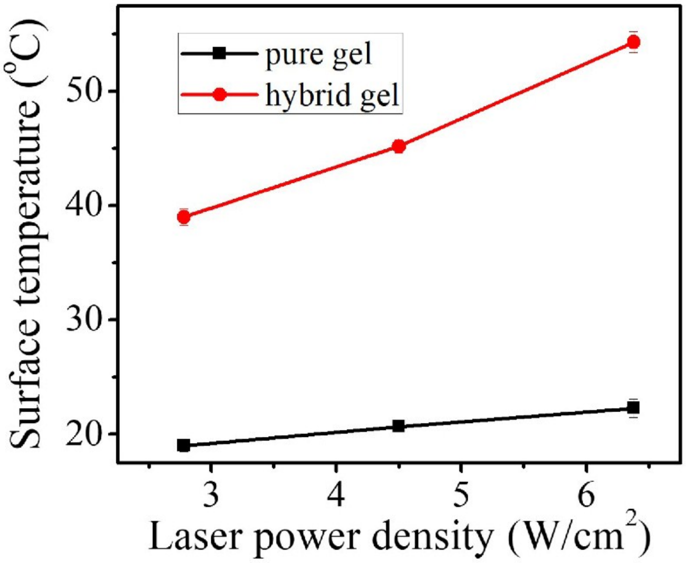

Fig. S8 Surface temperature of pure and hybrid PNIPAM hydrogel as a function of laser power density when irradiated in air. Room temperature is 18.5 ^{o}C.

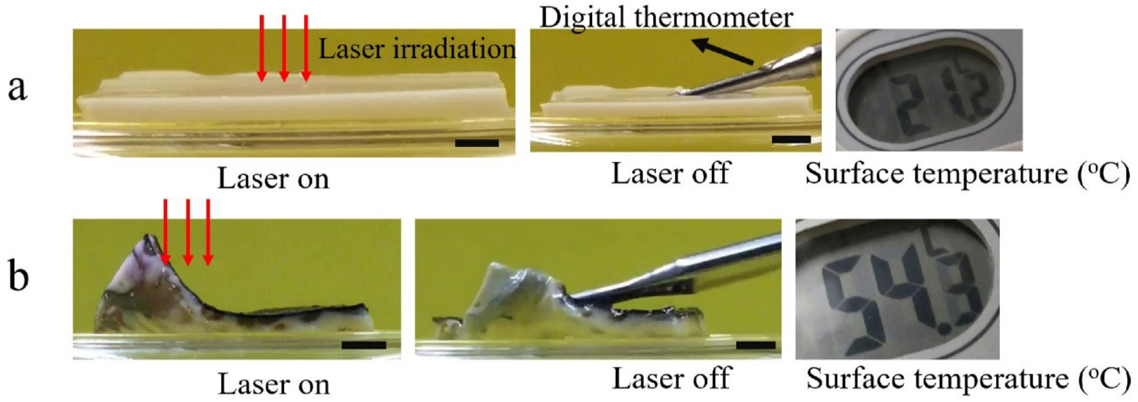

Fig. S9 Shape transformation of pure hydrogel (a) and hybrid hydrogel (b) in air under laser irradiation at 6.38W/cm^2. Thickness of hybrid gel layer in (b) is 200 μm. Scale bar: 4mm.

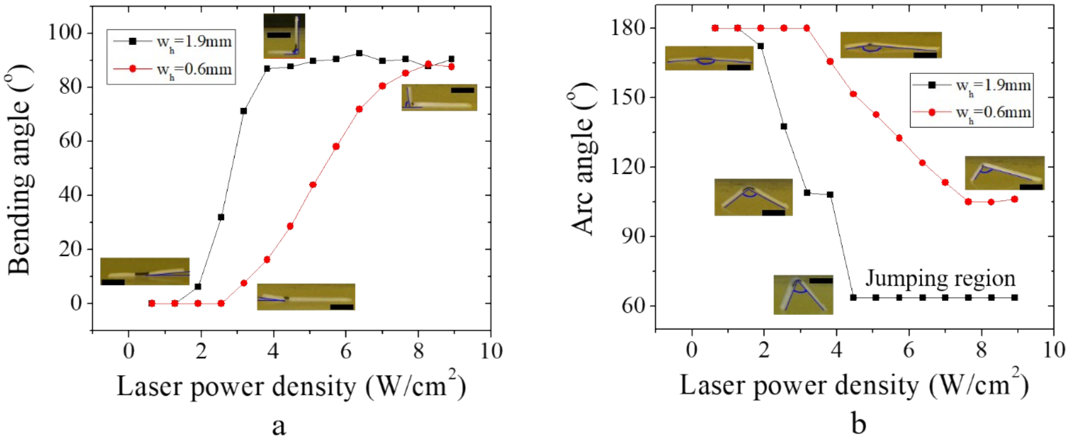

Fig. S10 Bending of composite hydrogel as a function of laser power density. w_h was the width of gold nanoparticle domain. The length of gold nanoparticle domain was 2.2mm. In a) the gold nanoparticle domain faced laser spot while in b) the nanoparticle domain faced away from the laser spot. Scale bar: 5mm.

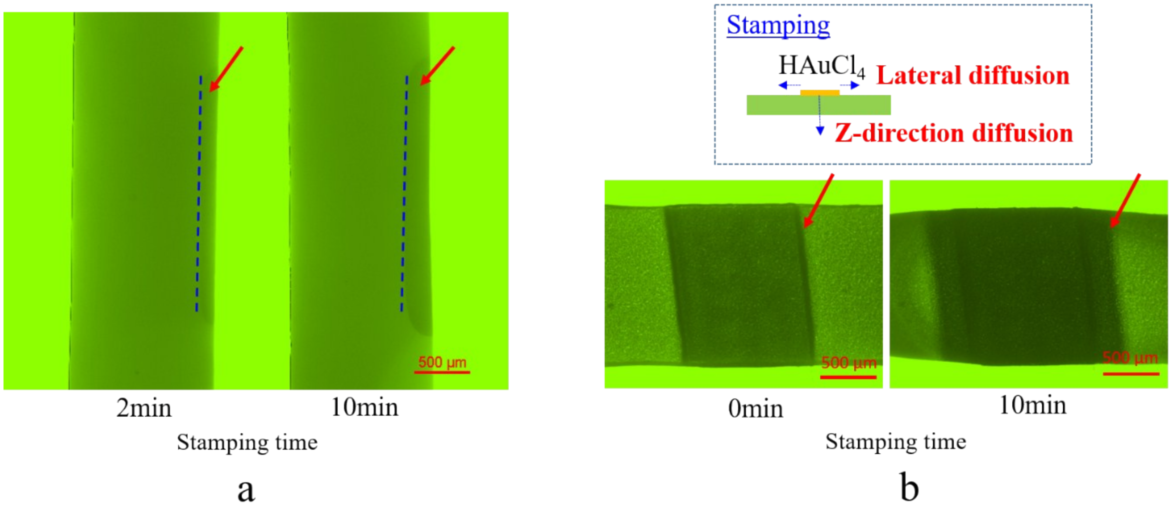

Fig. S11 Optical image showing diffusion-reaction process during stamping. The red arrow indicated the front of the gold nanoparticle domain generated during stamping.

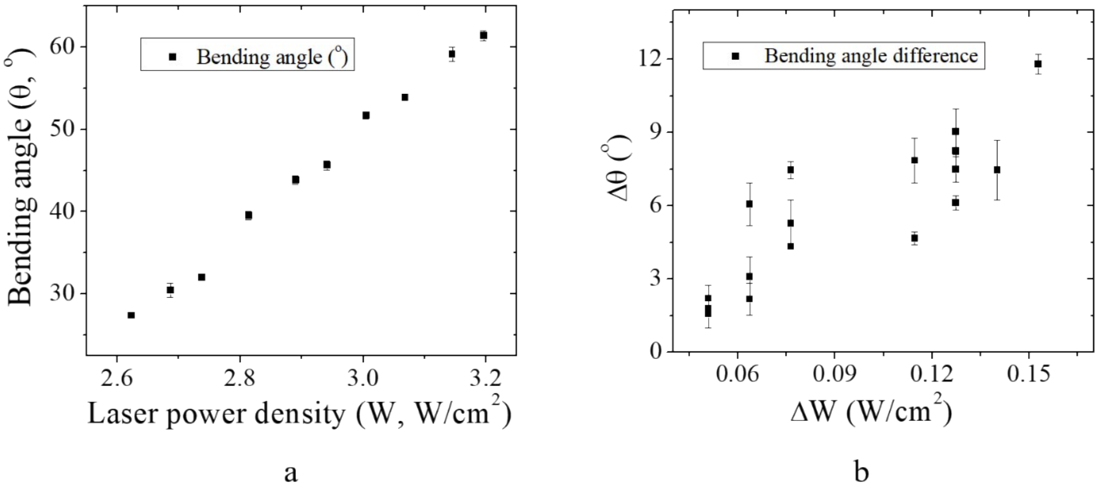

Fig. S12 Bending analysis of composite hydrogel as a function of laser power density. The gold nanoparticle domain had a width of 1.9mm, length of 2.2mm and thickness of 0.06mm. The total thickness of the hybrid hydrogel was 0.25mm.

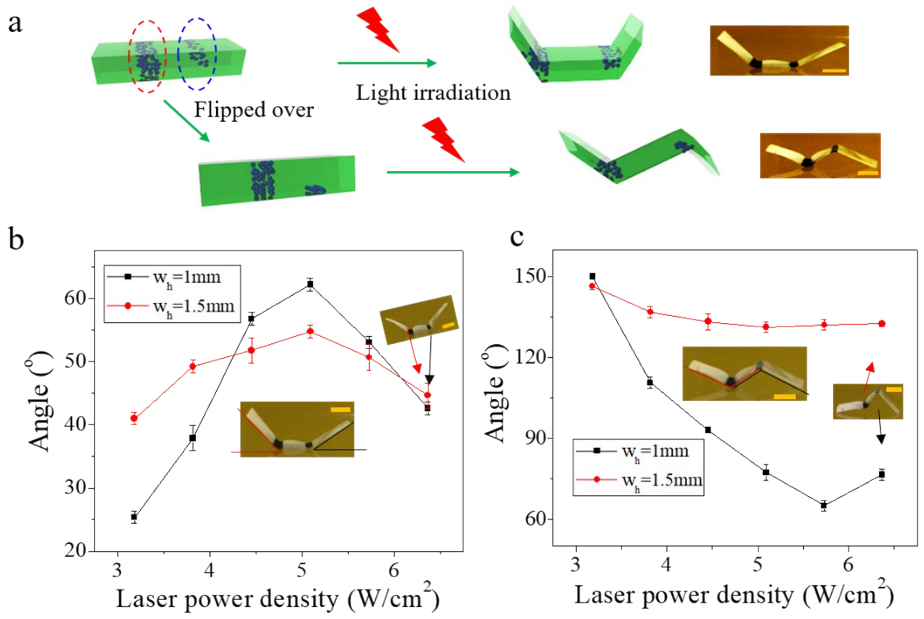

Fig. S13 Bending analysis of composite hydrogel with respect to laser irradiation direction. The composite hydrogel had two rectangular gold nanoparticle (AuNP) strips generated during one-time stamping process. One AuNP strip (w_h=1.5mm) penetrated through gel thickness, while the other one (w_h=1mm) only partially penetrated the gel.

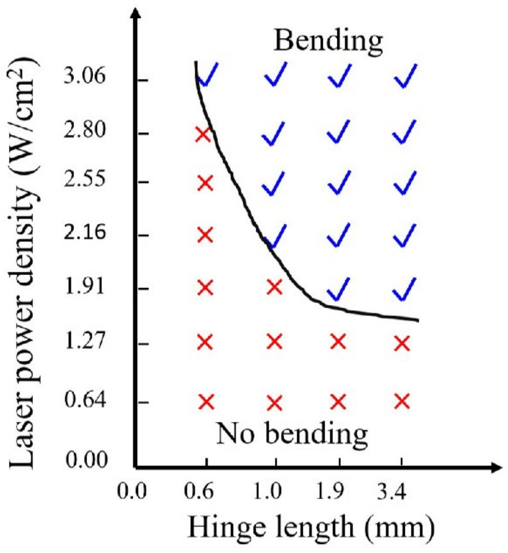

Fig. S14 Bending analysis of composite hydrogel sheet patterned with AuNP strip as hinge in its bending under laser irradiation. Length, width and thickness of composite hydrogel sheet are 20mm, 2.2mm and 0.25mm, respectively. The width of AuNP strip was 2.2mm, while its length varied.

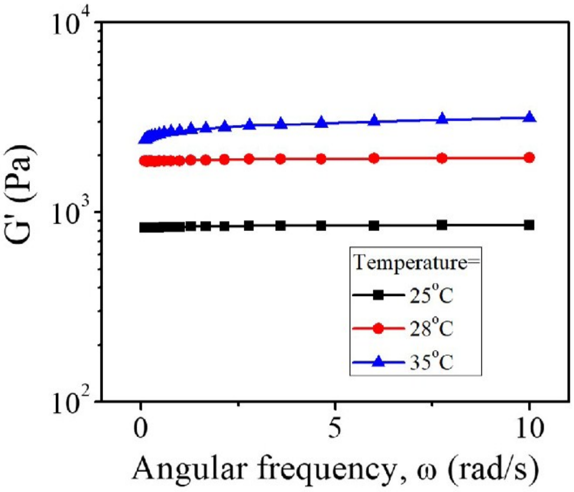

Fig. S15 Shear modulus of pure PNIPAM hydrogel as a function of temperature.

Table S1. Analysis of the minimum energy *E* (J) required for bending to occur.

Hinge length (*l*, mm)	Hinge width (*w*, mm)	Onset time for bending (*t*, s)	Minimum power density (I_o) needed (W/cm^2)	Minimum energy (E) required (J)
0.6	2.3	19	3.06	0.79
1.0	2.1	20	2.16	0.89
1.9	2.2	10	1.91	0.78
3.4	2.2	6	1.91	0.84

Table S2. Shear modulus of pure and hybrid gel layer as a function of temperature.

Temperature (°C)	Shear modulus (G′) of pure gel layer (Pa)	Shear modulus (G′) of hybrid gel layer (Pa)
25	838	2223
28	1879	2842
35	2675	3835

Table S3. Data used in study of effect of e on bending curvature of composite hydrogel sheet; h=0.3, h_{total}=0.25mm.

Temperature (T, °C)	Shear modulus of active gel layer (G, Pa)	Swelling ratio (ξ)
25	2223	3.28
28	2842	2.85
35	3835	0.78

Table S4. Calculation of bending curvature κ based on data in Table S2.

$e = \frac{G_{T,28}}{G_{T,25}}$	$\Delta\xi = \xi_{T,28}$	$A_{(T,28;\ T,25)}$	$\kappa_{(T,28;\ T,25)} = A\Delta\xi$	$e = \frac{G_{T,35}}{G_{T,25}}$	$\Delta\xi = \xi_{T,35} - \xi$	$A_{(T,35;\ T,25)}$	$\kappa_{(T,35;\ T,25)} = A\Delta\xi$
2.65	0.43	4.17	1.79	4.58	2.5	4.45	11.13

References

1. T. S. Rodrigues, A. G. M. da Silva, M. C. Gonçalves, H. V. Fajardo, R. Balzer, L. F. D. Probst, A. H. M. da Silva, J. M. Assaf, P. H. C. Camargo, *Langmuir* **2016,** *32*, 9371.